ELSEVIER

www.elsevier.nl/locate/jorganchem

Journal of Organometallic Chemistry 614–615 (2000) 83–91

Journal of Organometallic Chemistry

New Group 9 metal complexes containing *N*,*P*-chelate ligand system. Synthesis, characterization and application to catalytic hydrogenation

Heung-Sae Lee [a], Jin-Young Bae [a], Jaejung Ko [a,*1], Yong Soo Kang [b], Hoon Sik Kim [b,*2], Sung-Joon Kim [a], Jang-Hoon Chung [c], Sang Ook Kang [a,*3]

[a] *Department of Chemistry, Korea University, 208 Seochang, Chochiwon, Chung-nam 339-700, South Korea*
[b] *Korea Institute of Science and Technology, Cheongryangri, Seoul 130-650, South Korea*
[c] *Department of Chemistry, Myongji University, Yongin, Kyunggido 449-728, South Korea*

Received 28 January 2000

Dedicated to Professor Sheldon G. Shore on the occasion of his 70th birthday.

Abstract

New *N*,*P*-chelating *o*-carboranylaminophosphine ligand $Cab^{N,P}$ **2** [$Cab^{N,P} = o\text{-}C_2B_{10}H_{10}(CH_2NMe_2)(PPh_2)\text{-}N,P$] was prepared from *o*-carboranylamine $LiCab^N$ [$Cab^N = o\text{-}C_2B_{10}H_{10}(CH_2NMe_2)\text{-}N$] and chlorodiphenylphosphine. Consequently, the reaction of $[M(cod)(solv)_2]^+BF_4^-$ (M = Rh, Ir; cod = cycloocta-1,5-diene) with **2** was investigated. The resulting rhodium and iridium metal complexes $[(Cab^{N,P})M(cod)]^+BF_4^-$ **3** (M = Rh **3a**, Ir **3b**) were characterized by NMR spectroscopy and elemental analysis. In addition, an X-ray structure analysis was performed on complex **3a**, where the potential *N*,*P*-chelate ligand **2** was found to coordinate in a bidentate mode. The subsequent reaction of **3** with PPh_3 and CO resulted in the dissociation of the *N*,*P*-chelate ligand **2** to yield the penta-coordinate metal complexes $[(PPh_3)_2M(CO)_3]^+BF_4^-$ **4** (M = Rh **4a**, Ir **4b**). The structure of **4a** was determined by X-ray diffraction analysis, exhibiting a trigonal bipyramidal configuration with the triphenylphosphine ligands occupying axial positions. The activities of complex **3** as a catalyst precursor during the hydrogenation of cyclohexene were tested and produced the cyclohexane with 100% conversion in the case of **3a**.

Keywords: Chelate; Rhodium; Iridium; *o*-Carborane; Catalyst precursor; Hydrogenation

1. Introduction

In recent years, transition metal complexes with ligands containing dissimilar donor atoms such as phosphorous and nitrogen have been widely investigated, primarily for their applications in important homogeneous catalytic processes [1]. Therefore, the design of such ligand systems containing one functional group strongly bound to a late transition metal and another coordinatively labile has been of considerable interest [2]. The *N*,*P*-chelate ligand **2** described in this work having an *ortho*-substituent bearing an amino group can generate a six-membered chelate ring by coordination through the nitrogen and phosphorus to a metal center. In addition, phosphine ligands possessing an *o*-carboranyl group deserve particular attention, and influence of this group as a rigid ligand backbone [3] in six-membered metal chelates on the hydrogenation has been studied.

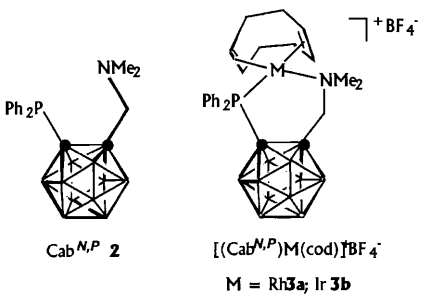

$Cab^{N,P}$ **2** $[(Cab^{N,P})M(cod)]^+BF_4^-$ M = Rh **3a**; Ir **3b**

[1]* Corresponding author.
[2]* Corresponding author.
[3]* Corresponding author. Fax: +82-415-8675396; sangok@tiger.korea.acr

0022-328X/00/$ - see front matter
PII: S0022-328X(00)00607-0

The use of *o*-carborane as the ligand backbone is rare in catalytic reactions, while the *nido*-$\{C_2B_9\}$ complex has been proven to be a useful ancillary ligand for catalytic hydrogenation reactions [4]. This ligand **2** is chosen because it has an arylphosphine at one end to stabilize the metal ion in a low oxidation state and a weakly coordinating amine function at the other end which will readily be substituted by an incoming π-acceptor ligand.

In order to investigate the influence of the *N*,*P*-chelate ligand **2** on the catalyst behavior of the complex in the hydrogenation reaction, we have synthesized and characterized the rhodium and iridium complexes **3**. In particular, complex **3a** was successfully applied as a homogeneous catalyst for the hydrogenation of cyclohexene and its catalytic activity is discussed.

2. Results and discussion

2.1. Preparation and characterization of $Cab^{N,P}$ 2

The reaction of the *o*-carboranylamine $HCab^N$ 1 with 1.1 equivalent of BuLi followed by the addition of one equivalent of chlorodiphenylphosphine in THF at low temperature (Scheme 1) results in the formation of the corresponding *o*-carboranylaminophosphine $Cab^{N,P}$ **2** in good yield (65%).

The pure form of complex **2** is a yellowish, off-white powder which, although slightly hygroscopic, can be handled safely in air. Complex **2** is readily soluble in Et_2O and THF and is somewhat less soluble in benzene and toluene. The composition of the new complexes **2** has been unequivocally established by elemental analysis. The ^{1}H- and ^{13}C-NMR data are in agreement with the proposed cage structure and confirm the presence of phosphino and amino groups at the cage 1- and 2-positions, respectively. The ^{1}H-NMR data contain phenyl resonances (7.24–7.82 ppm) for the cage 1-position and a methyl resonance (2.30 ppm) and a methylene resonance (3.32 ppm) for the dimethylamino substituent. The compound shows only a single ^{31}P-NMR signal; these and other NMR (^{1}H, ^{11}B, and ^{13}C) spectroscopic data are consistent with the described *N*,*P*-chelate structure, which has been determined by X-ray crystallographic studies. Table 1.

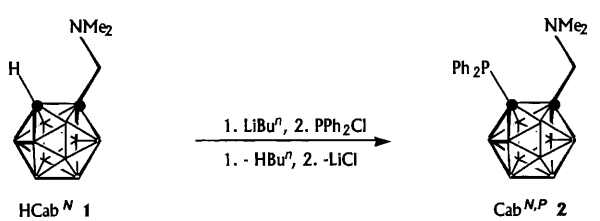

Scheme 1.

2.2. X-ray diffraction structure of the N,P-chelate ligand $Cab^{N,P}$ 2

The molecular structure and atom-labeling scheme for complex **2** are shown in Fig. 1; whereas, selected bond distances (Å) and angles (°) are presented in Table 2. The observed conformation of **2** ligand in the solid state is nearly ideal for a bidentate *N*,*P*-chelate ligand. The phosphorous and nitrogen lone-pair vectors are nearly parallel and approximately face each other in the solid state. Two carbon atoms of two phenyl groups and one carbon atom of the cage are bonded to a phosphorus atom in a pyramidal arrangement. The P–C bond lengths of 1.828(2)–1.887(2) Å and C–P–C angles of 100.6(1)–107.7(1)° are similar to those in 1-PPh_2-2-Me–$C_2B_{10}H_{10}$ [5]. The two carbon atoms of the two methyl groups and one carbon atom of the methylene unit are bonded to a nitrogen atom in a pyramidal arrangement. The intercage boron–boron (1.77–1.79 Å) and boron–carbon (1.71–1.73 Å) distances are normal, and the carbon–carbon distance between the only adjacent carbons, C(1)–C(2) 1.689(3) Å, is also in the range previously observed in other *o*-carborane cage systems [6].

2.3. Reactions of 2 with $[M(cod)(solv)_2]^+BF_4^-$ (M = Rh, Ir; cod = cycloocta-1,5-diene)

The *N*,*P*-chelate metal complexes **3a**,**b** were prepared by reactions between the cationic complexes $[M(cod)(solv)_2]^+BF_4^-$ and a slight excess of the corresponding *N*,*P*-chelate ligand **2** (Scheme 2). Isolation of the pure products, which ranged in color from yellow to orange, was achieved by recrystallization. Typically, the yields of **3a**,**b** were on the order of 72–75%.

The elemental analysis results show that the air–stable complexes **3a**,**b** have compositions corresponding to a 1:1 metal complex of the M(cod) fragment and *o*-carboranylaminophosphine **2**. The ^{1}H-NMR spectra of **3a**,**b** show signals for the cyclooctadiene ligand at 2.18–2.58 (methylene protons) and at 5.45–5.50 ppm (olefinic protons). In the ^{1}H- and ^{13}C{^{1}H}-NMR spectra of **3**, the N–Me resonances are shifted to low field compared to the corresponding resonance in the free ligand. This observation is strong evidence for M–N coordination [7]. The complex **3a** is characterized by ^{31}P{^{1}H}-NMR spectroscopy with a doublet at 52.63 ppm and $J_{Rh\text{-}P}$ coupling constant of 166.5 Hz, typical for $[Rh(cod)(PR_3)_2]^+$ [8] or $[Rh(cod)(P\text{-}N)]^+$ [9] compounds. A detailed analysis of the spectroscopic data (^{1}H-NMR, ^{11}B-NMR, ^{13}C-NMR, and IR spectra) showed that the *N*,*P*-chelate ligand **2** is coordinated to the metal(I) ion through the nitrogen and phosphorous atoms. In addition, the spectroscopic data of chelates **3a**,**b** suggest a fluxional process [10] within the molecules. This fluxionality could be due to inversion at

Table 1
X-ray crystallographic data and processing parameters for compounds **2**, **3a**·CH_2Cl_2, and **4a**·CH_2Cl_2

	2	**3a**·CH_2Cl_2	**4a**·CH_2Cl_2
Formula	$C_{17}H_{28}B_{10}NP$	$C_{26}H_{42}B_{11}Cl_2F_4NPRh$	$C_{40}H_{30}B_{11}Cl_2F_4O_3P_2Rh$
Formula weight	385.47	768.30	881.239
Crystal system	Monoclinic	Monoclinic	Monoclinic
Space group	$P2_1/n$ (no. 14)	$P2_1/c$ (no. 14)	$P2_1/n$ (no. 14)
Z	4	4	4
Cell constants			
a (Å)	9.8428(4)	12.8745(7)	17.0197(9)
b (Å)	21.103(2)	13.3315(6)	13.921(1)
c (Å)	11.7825(1)	20.6958(1)	17.3040(9)
β (°)	112.863(6)	90.977(5)	104.285(5)
V (Å^3)	2255.1(2)	3551.6(3)	3973.0(5)
μ (cm^{-1})	0.126	0.718	0.614
Crystal size (mm)	$0.30\times0.50\times0.55$	$0.30\times0.40\times0.45$	$0.50\times0.45\times0.50$
D_{calc} (g cm^{-3})	1.135	1.437	1.473
F(000)	808	1560	1692
Radiation	Mo–K_α	Mo–K_α	Mo–K_α
Wavelength (Å)	0.7170	0.7170	0.7170
θ Range (°)	1.93–25.97	1.58–25.97	1.50–25.97
h, k, l collected	$+12, +26, \pm 14$	$+15, +16, \pm 25$	$+20, +17, \pm 21$
Reflections measured	4697	7144	8074
Unique reflections	4402	6818	7768
Reflections used in refinement [$I>2\sigma(I)$]	3121	5093	5857
Parameters	284	437	481
Data/parameter ratio	15.5	15.60	16.15
[a]R_1	0.0492	0.0555	0.0708
[b]wR_2	0.1443	0.1592	0.2058
Goodness-of-fit on F^2	1.076	1.294	0.797

[a] $R_1 = \Sigma\,||F_o|-|F_c||/\Sigma\,|F_o|$ (based on reflections with $F_o^2 > 2\sigma F_o^2$).
[b] $wR_2 = [\Sigma\,[w(F_o^2-F_c^2)^2]/\Sigma\,[w(F_o^2)^2]]^{1/2}$; $w = 1/[\sigma^2(F_o^2)+(0.095P)^2]$; $P = [\max(F_o^2, 0)+2F_c^2]/3$ (also with $F_o^2 > 2\sigma F_o^2$).

the nitrogen atom and this would account for the absence of a diastereotopic AB pattern for the NCH_2 protons. The above spectral data suggest that the *N*,*P*-chelates **3a**,**b** have the structure shown in Scheme 2. Confirmation of this structure came from a single-crystal X-ray structure determination.

2.4. X-ray diffraction structure of the N,P-chelate metal complex *3a*

The molecular structure of **3a** is shown in Fig. 2, and a listing of selected bond lengths and angles for **3a** can be found in Table 2. The crystal structure shows that coordination around the rhodium atom is approximately square–planar. The carborane cage is bidentately coordinated through N and P atoms to the Rh(I) ion, while the cod is η^4-coordinated to the metal. The molecular structure of **3a** is similar to that of $[(cod)M(DIPOF)]^+BF_4^-$ (M = Rh [11], Ir [1]) (DIPOF = oxazolinylferrocenyldiphenylphosphine). The Rh–P and Rh–N bond lengths are in the range usually found in this family of complexes [12]. The average Rh–C(cod) distance *trans* to the phosphorous is 2.256(5) Å, which is a normal value for Rh(I) complexes containing cod ligands *trans* to P donor atoms [12]. On the contrary, the average Rh–C(cod) distance *trans* to nitrogen is 2.138(5) Å, which is comparable to that in Rh(I) complexes with a *trans* N donor ligand [12]. Thus, the Rh–C(cod) distance *trans* to phospho-

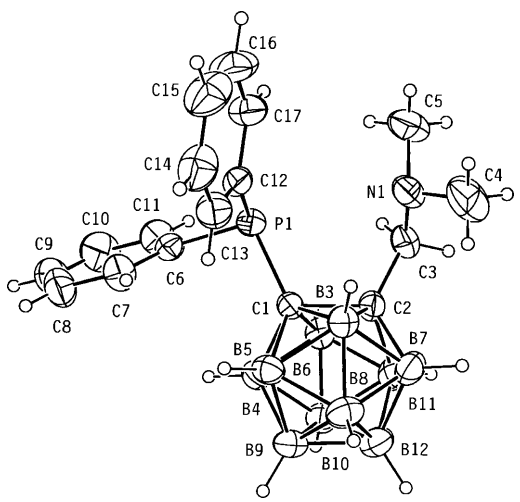

Fig. 1. Molecular structure of $Cab^{N,P}$ 2. The thermal ellipsoids are drawn at the 30% probability level.

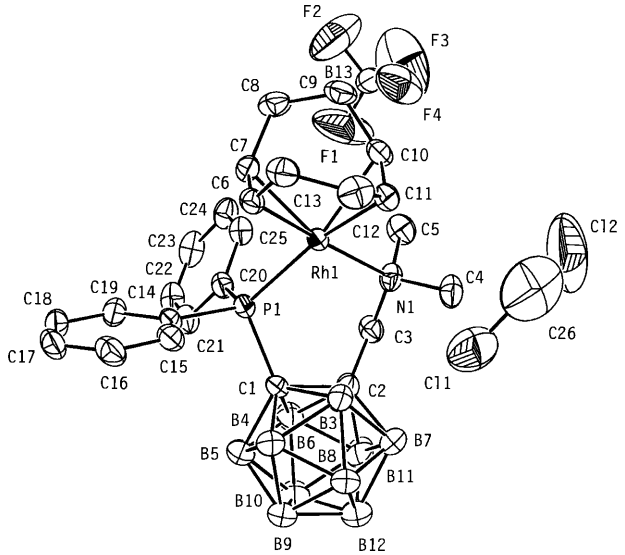

Fig. 2. Molecular structure of $[(Cab^{N,P})Rh(cod)]^+BF_4^-$ **3a**·CH_2Cl_2. The thermal ellipsoids are drawn at the 30% probability level.

rous is longer than that *trans* to nitrogen. A higher contribution by back-donation is found in the alkene fragment of cod *trans* to nitrogen. The six-membered Rh–P–C–C–C–N ring is non-planar, with the dihedral angles between the planes defined by [Rh(1), P(1), C(3), N(1)] and [P(1), C(1), C(2), C(3)] being 52.8(2)° The sum of the angles [361.2(2)°] around Rh formed by the coordinated N and P atoms and the midpoints of the double-bond carbon atoms of cod indicates the planarity of the (*N*,*P*)Rh(diene) moiety. The bond lengths and angles associated with cod and the coordinated *o*-carboranylaminophosphine **2** are normal with respect to the other *o*-carboranyl substituted compounds [6].

2.5. Reaction of *3* with CO and PPh_3

The *N*,*P*-chelate metal complex **3** is of direct relevance to homogeneous catalysis since the weakly coordinated end of the chelate should undergo ready displacement by incoming π-acceptor ligands. To understand the coordination behavior and reactivity of **3**, we have studied its reactivity toward π-acceptor ligands. CO was bubbled, at r.t. and 1 atm through a CH_2Cl_2 solution containing **3** and PPh_3 (1:2). The compound $[(PPh_3)_2M(CO)_3]^+BF_4^-$, 4 (M = Rh **4a**, Ir **4b**), was almost quantitatively formed. A structure in which the phosphorus atoms of PPh_3 are *trans* to each other was assigned on the basis of the $^{31}P\{^1H\}$-NMR spectrum. However, to confirm this analysis, we determined the crystal structure of **4a**. It has been shown that a dimethylamino arm of a chelate coordinated to rhodium(I) can readily be displaced by CO, and synthetic and kinetic studies have shown that a similar reaction occurs with other low-valent metals [2,13] (Scheme 3).

We attribute these results to a reaction sequence whose first step involves M–N bond breaking to form a three-coordinate species. With two relatively strong donor ligands, PPh_3 and CO, M–P dissociation is most likely, and thus, five-coordinate complexes **4** are generated [14]. We have direct evidence for M–L bond breaking (L = N or P donor); therefore, a sequence related to ours has been postulated in $[(cod)M(ODIPNAP)]^+BF_4^-$ (M = Rh, Ir) (ODIPNAP = oxazolinyldiphenylphosphinobinaphthalene) [1b].

2.6. X-ray diffraction structure of *4a*

The molecular structure of **4a** is shown in Fig. 3, and a listing of selected bond lengths and angles for **4a** can be found in Table 2. The crystal structure shows that coordination around the rhodium atom is approximately trigonal-bipyramidal. The $[Rh(CO)_3(PPh_3)_2]^+$ cation is associated with the mutually *trans* Rh–P distances Rh(1)–P(1) = 2.352(2) and Rh(1)–P(2) = 2.356(2) Å, with an interligand angle of of P(1)–Rh(1)–P(2) = 177.53(6)°. The equatorial carbonyl ligands have Rh–CO linkages defined by Rh(1)–C(1) = 1.939(8), Rh(1)–C(2) = 1.949(8), and Rh(1)–C(3) = 1.972(8) Å. The Rh–C–O systems are close to linear (178.0(9)–178.2(8)°) with a C–O distance of 1.11(1)–1.12(1) Å. Angles between the equatorial ligands show some deviation from D_{3h} symmetry with C(1)–Rh(1)–C(3) = 116.6(4)° as compared to C(1)–Rh(1)–C(2) = 120.0(4) and C(2)–Rh(1)–C(3) = 123.4(4)°. The axial–equatorial

Table 2
Selected interatomic distances (Å) and angles (°) in **2**, **3a**·CH_2Cl_2, and **4a**·CH_2Cl_2

Bond Distances in ***2***			
P(1)–C(12)	1.828(2)	P(1)–C(6)	1.832(2)
P(1)–C(1)	1.887(2)	N(1)–C(3)	1.440(3)
N(1)–C(4)	1.448(4)	N(1)–C(5)	1.464(4)
C(1)–C(2)	1.689(3)		
Bond Angles in ***2***			
C(12)–P(1)–C(6)	103.3(1)	C(12)–P(1)–C(1)	107.7(1)
C(6)–P(1)–C(1)	100.6(1)	C(3)–N(1)–C(4)	112.0(2)
C(3)–N(1)–C(5)	110.1(2)	C(4)–N(1)–C(5)	109.6(3)
C(2)–C(1)–P(1)	113.7(1)	B(4)–C(1)–P(1)	129.5(2)
C(3)–C(2)–C(1)	118.6(2)		
Bond Distances in ***3a***·CH_2Cl_2			
Rh(1)–C(7)	2.119(5)	Rh(1)–C(6)	2.156(5)
Rh(1)–C(11)	2.232(5)	Rh(1)–C(10)	2.280(5)
Rh(1)–N(1)	2.300(4)	Rh(1)–P(1)	2.306(3)
P(1)–C(20)	1.801(6)	P(1)–C(14)	1.827(5)
P(1)–C(1)	1.892(5)	N(1)–C(3)	1.480(7)
N(1)–C(4)	1.484(7)	N(1)–C(5)	1.498(7)
C(1)–C(2)	1.676(7)	C(2)–C(3)	1.521(8)
C(6)–C(7)	1.408(8)	C(6)–C(13)	1.520(8)
C(7)–C(8)	1.503(8)	C(8)–C(9)	1.518(9)
C(9)–C(10)	1.500(8)	C(10)–C(11)	1.395(8)
C(11)–C(12)	1.499(8)	C(12)–C(13)	1.516(9)
Bond Angles in ***3a***·CH_2Cl_2			
C(7)–Rh(1)–C(6)	38.4(2)	C(7)–Rh(1)–C(11)	95.4(2)
C(6)–Rh(1)–C(11)	78.6(2)	C(7)–Rh(1)–C(10)	79.7(2)
C(6)–Rh(1)–C(10)	86.0(2)	C(11)–Rh(1)–C(10)	36.0(2)
C(7)–Rh(1)–N(1)	145.6(2)	C(6)–Rh(1)–N(1)	174.0(2)
C(11)–Rh(1)–N(1)	95.8(2)	C(10)–Rh(1)–N(1)	90.8(2)
C(7)–Rh(1)–P(1)	89.8(2)	C(6)–Rh(1)–P(1)	91.8(2)
C(11)–Rh(1)–P(1)	156.7(2)	C(10)–Rh(1)–P(1)	165.7(2)
N(1)–Rh(1)–P(1)	92.6(1)	C(20)–P(1)–C(14)	104.6(2)
C(20)–P(1)–C(1)	107.3(2)	C(14)–P(1)–C(1)	101.9(2)
C(1)–P(1)–Rh(1)	109.3(2)	C(3)–N(1)–C(4)	109.8(4)
C(3)–N(1)–C(5)	103.5(4)	C(4)–N(1)–C(5)	107.6(5)
C(3)–N(1)–Rh(1)	115.1(3)	C(2)–C(1)–P(1)	112.8(3)
C(3)–C(2)–C(1)	118.7(4)	N(1)–C(3)–C(2)	119.1(5)
Rh(1)–C(1)	1.939(8)	Rh(1)–C(2)	1.949(8)
Rh(1)–C(3)	1.972(8)	Rh(1)–P(1)	2.352(2)
Rh(1)–P(2)	2.356(2)	P(1)–C(10)	1.813(7)
P(1)–C(16)	1.817(7)	P(1)–C(4)	1.820(7)
P(2)–C(22)	1.816(7)	P(2)–C(34)	1.818(7)
P(2)–C(28)	1.818(7)	O(1)–C(1)	1.12(1)
O(2)–C(2)	1.11(1)	O(3)–C(3)	1.11(1)
Bond Angles in ***4a***·CH_2Cl_2			
C(1)–Rh(1)–C(2)	120.0(4)	C(1)–Rh(1)–C(3)	116.6(4)
C(2)–Rh(1)–C(3)	123.4(4)	C(1)–Rh(1)–P(1)	91.1(2)
C(2)–Rh(1)–P(1)	88.3(2)	C(3)–Rh(1)–P(1)	90.6(2)
C(1)–Rh(1)–P(2)	90.6(2)	C(2)–Rh(1)–P(2)	89.3(2)
C(3)–Rh(1)–P(2)	90.3(2)	P(1)–Rh(1)–P(2)	177.53(6)
C(10)–P(1)–C(16)	104.8(3)	C(10)–P(1)–C(4)	105.8(3)
C(16)–P(1)–C(4)	103.9(3)	C(10)–P(1)–Rh(1)	114.3(2)
C(16)–P(1)–Rh(1)	114.4(2)	C(4)–P(1)–Rh(1)	112.6(2)
C(22)–P(2)–C(34)	105.6(3)	C(22)–P(2)–C(28)	103.9(3)
C(34)–P(2)–C(28)	106.0(3)	C(22)–P(2)–Rh(1)	112.5(2)
C(34)–P(2)–Rh(1)	114.5(2)	C(28)–P(2)–Rh(1)	113.3(2)
O(1)–C(1)–Rh(1)	178.2(8)	O(2)–C(2)–Rh(1)	178.0(9)
O(3)–C(3)–Rh(1)	178.2(8)		

angles are close to 90°, ranging from P(1)–Rh(1)–C(2) = 88.3(2) to P(1)–Rh(1)–C(1) = 91.1-(2)°. The Rh–P–C angles are all expanded from the ideal tetrahedral value (range 112.5(2)–114.5(2)°) and the C(*ipso*)–P–C(*ipso′*) angles are all compressed (range 103.9(3)–106.0(3)°); P–C distances range from P(1)–C(10) = 1.813(7) to P(1)–C(4) = 1.820(7) Å. It is similar to that observed in the isoelectronic Ir(I) species $[Ir(CO)_3(PPh_3)_2]^+[HSO_4]^-$ $1/3H_2O$ [15], in which the average distances are Ir–P = 2.643(3) and Ir–CO = 1.93(1) Å.

2.7. Catalytic hydrogenation of cyclohexene

The results of the hydrogenation of cyclohexene catalyzed by cationic rhodium(I) and iridium(I) complexes containing the *N*,*P*-chelate ligand **2** are shown in Table 3. The presence of the *N*,*P*-chelate ligand in the rhodium(I) catalyst allows good catalytic activity during the hydrogenation of cyclohexene (Scheme 4).

The yield of the catalytic hydrogenation was largely dependent upon the reaction solvents. With the rhodium(I) complex **3a**, the yield was increased in a polar methanol solvent. Thus, the hydrogenation of cyclohexene with the catalyst precursor **3a** proceeds with 100% conversion operating at 20 atm (H_2) and 80°C for 50 min in methanol. On the contrary, employment of the iridium complex **3b** resulted in 52.8% yield under the same conditions. However, a better yield was observed with **3b** in 1,2-dichloroethane (90.0% conversion at 80°C). Based on this result, $Cab^{N,P}$ 2 was found to be a useful ligand in the hydrogenation of cyclohexene.

Compound **2** is representative of a series of easily accessible chelating ligand in which the two heteroatoms can be independently introduced in consecutive synthetic steps. Such a preparation warrants great flexibility, and the approach should allow fine tuning of the ligands, with respect to both their steric and their electronic properties. Work directed towards the extension of the different ligands and further applications in catalytic reactions is in progress.

3. Experimental

3.1. General considerations

All manipulations were performed under a dry, oxygen-free, nitrogen or argon atmosphere using standard Schlenk techniques or in a Vacuum Atmosphere HE-493 dry box. THF was freshly distilled over potassium benzophenone. Ether and toluene were dried and distilled from sodium benzophenone. Dichloromethane and hexane were dried and distilled over CaH_2. ^{11}B-, ^{13}C-, ^{1}H-, and ^{31}P-NMR spectra were recorded on a Varian Gemini 2000 spectrometer operating at 64.2,

50.3, 200.1, and 80.0 MHz, respectively. All boron-11 chemical shifts were referenced to BF_3Et_2O (0.0 ppm) with a negative sign indicating an upfield shift. All proton and carbon chemical shifts were measured relative to internal residual chloroform from the lock solvent (99.5% $CDCl_3$) and then referenced to Me_4Si (0.00 ppm). The ^{31}P-NMR spectra were recorded with 85% H_3PO_4 as an external standard. IR spectra were recorded on a Biorad FTS-165 spectrophotometer. Elemental analyses were performed with a Carlo Erba Instruments CHNS-O EA1108 analyzer. All the melting points recorded are uncorrected. Decaborane and 1-dimethylaminoprop-2-yne were purchased from the Callery Chemical Co. and Aldrich, respectively, and were used without purification. The following starting materials were prepared according to literature procedures: $HCab^N$ 1 [16], $[Rh(\mu\text{-}Cl)(cod)]_2$ [17], and $[Ir(\mu\text{-}Cl)(cod)]_2$ [18].

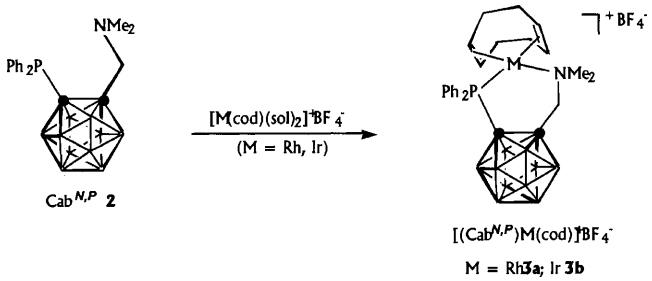

Scheme 2.

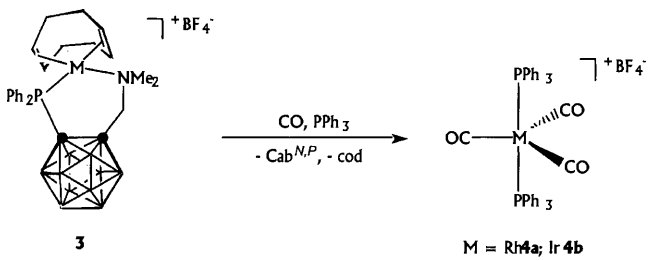

Scheme 3.

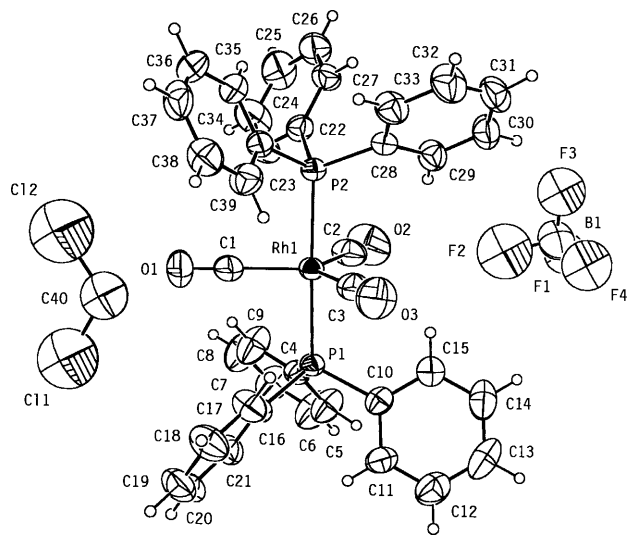

Fig. 3. Molecular structure of $[(PPh_3)_2Rh(CO)_3]^+BF_4^-$ **4a**·CH_2Cl_2. The thermal ellipsoids are drawn at the 30% probability level.

3.2. Synthesis of $Cab^{N,P}$ 2

A solution of $HCab^N$ 1 (0.60g, 3.0 mmol) in THF (30 ml) was treated with 1.6 M hexane solution of Bu^{n}Li (2 ml, 3.2 mmol) at −78°C. After stirring at −78°C for 2 h, the reaction mixture was treated with chlorodiphenylphosphine (0.66 g, 3.0 mmol), warmed to r.t., and then stirred for a further 12 h to complete the reaction. The solvent was removed under reduced pressure, and the residue was extracted with a small amount of methylene chloride. The extract was loaded on a silica gel column and eluted with a mixture of hexane and benzene (2:3). The colorless band first eluted was collected, and the solvents were removed in vacuo to give **2** as a white powder (0.75 g, 1.94 mmol, 65%). ^{11}B-NMR (64.2 MHz, ppm, C_6D_6); −1.26 (*d*, 1B, $J_{BH} = 190$ Hz), −4.58 (*d*, 1B, $J_{BH} = 160$ Hz), −10.43 (*d*, 8B, $J_{BH} = 110$ Hz). ^{1}H-NMR (200.13 MHz, ppm, C_6D_6) 7.82 (*m*, 4H, PPH), 7.45 (*m*, 4H, PPH), 7.24 (*m*, 2H, PPH), 3.32 (*d*, 2H, CH_2, 2.60 Hz), 2.30 (*s*, 6H, NMe); ^{13}C-NMR (50.3 MHz, ppm, $CDCl_3$) 135.31 (PPH), 131.42 (PPH), 128.65 (PPH), 62.83 (*s*, 1C, CH_2), 46.2 (*s*, 2C, NMe). ^{31}P{^{1}H}-NMR (80.0 MHz, ppm, C_6D_6): −19.36 (*s*, PPh_2). Anal. Calc. for $C_{17}H_{28}B_{10}NP$: C, 52.97; H, 7.32; N, 3.63. Found: C, 53.01; H, 7.36; N, 3.59%. $R_f = 0.96$ by silica gel TLC analysis (benzene), m.p. = 114°C. IR spectrum (KBr pellet, cm^{-1}) 3070 (w), 3055 (w), 2955 (w), 2930 (w), 2820 (w), 2649 (w), 2610 (s), 2590 (s), 2555 (s), 2550 (s), 1475 (m), 1465 (m), 1449 (m), 1435 (s), 1376 (w), 1304 (w), 1264 (w), 1157 (w), 1092 (m), 1071 (m), 1049 (w), 1027 (m), 1000 (w), 862 (m), 748 (s), 741 (s), 697 (s), 542 (w), 499 (s).

3.3. Synthesis of **3a**

To a solution of $[Rh(cod)Cl]_2$ (0.12 g, 0.24 mmol) in THF (5 ml) was added $AgBF_4$ (0.10 g, 0.51 mmol). The immediate formation of AgCl occurred as indicated by a white precipitate. The reaction mixture was stirred vigorously for 1 h. The cloudy gray reaction mixture was filtered through a fine frit with Celite to give a yellow filtrate. The *N*,*P*-chelate ligand **2** (0.20 g, 0.52 mmol) was then added, and the resulting solution was magnetically stirred at r.t. for 1 h. When diethyl ether (10 ml) was added to the solution, **3a** precipitated as an orange solid, which was collected by filtration and dried under vacuum: 0.25 g (0.37 mmol), 75% isolated yield. ^{11}B-NMR (64.2 MHz, ppm, $CDCl_3$); −1.65 (*s*, 1B, BF_4), −4.73 (*d*, 2B, $J_{BH} = 150$ Hz), −7.88 (*d*, 4B, $J_{BH} = 160$ Hz), −10.39 (*d*, 4B, $J_{BH} = 160$ Hz). ^{1}H-

Table 3
Catalytic hydrogenation of cyclohexene [a]

Entry	Catalyst	Solvent	Reaction Time (min)	% Conversion	Product
1	**3a**	Methanol	50	100.0	Cyclohexane
2	**3b**	Methanol	50	52.8	Cyclohexane
3	Willkinson's catalyst	Methanol	50	59.2	Cyclohexane
4	**3a**	1,2–Dichloro ethane	50	98.8	Cyclohexane
5	**3b**	1,2–Dichloro ethane	50	90.0	Cyclohexane
6	Willkinson's catalyst	1,2–Dichloro ethane	50	87.4	Cyclohexane
7	**3a**	Toluene	50	84.7	Cyclohexane
8	**3b**	Toluene	50	17.4	Cyclohexane
9	Willkinson's catalyst	Toluene	50	98.1	Cyclohexane

[a] Experimental conditions: 80°C; 300 psi (H_2); [Cyclohexene]/[Catalyst] = 1219.

NMR (200.13 MHz, ppm, $CDCl_3$) 7.96 (*m*, 4H, PPH), 7.71 (*m*, 6H, PPH), 5.50 (br *s*, 4H = CH cod), 3.08 (*d*, 2H, N–CH_2, 2.60 Hz), 2.88 (*s*, 6H, NMe), 2.54 (br *s*, 4H, CH_{exo} cod), 2.18 (br *s*, 4H, CH_{endo} cod). $^{13}C\{^1H\}$-NMR (50.3 MHz, ppm, $CDCl_3$) 137.83 (PPH), 135.05 (PPH), 131.82 (PPH), 67.22 (*s* = CH cod), 60.46 (*s*, N–CH_2), 55.02 (*s*, NMe), 17.42 (*s*, CH_2 cod). $^{31}P\{^1H\}$-NMR (80.0 MHz, ppm, $CDCl_3$): 52.63 (*s*, PPh_2, J_{Rh-P} = 166.5 Hz); Anal. Calc. for $C_{25}H_{40}B_{11}F_4NPRh$: C, 43.94; H, 5.90; N, 2.05. Found: C, 43.96; H, 5.94; N, 2.08%. Mp = 190–192°C (dec.). IR spectrum (KBr pellet, cm^{-1}) 3063 (w), 2970 (w), 2879 (w), 2657 (w, sh), 2613 (s, sh), 2575 (s), 1478 (m), 1436 (s), 1415(w), 1318 (w), 1183 (w), 1089 (s), 1054 (vs), 1037 (s), 998 (m), 853 (w), 788 (w), 739 (m), 698 (m), 519 (w), 504 (s).

3.4. Synthesis of $[(Cab^{N,P})Ir(cod)]^+BF_4^-$ *3b*

A similar procedure was employed as described above but with the following quantities: $[Ir(cod)Cl]_2$ (0.17 g, 0.25 mmol); $AgBF_4$ (0.10 g, 0.51 mmol); **2** (0.20 g, 0.52 mmol). An orange solid of **3b** was isolated as described for the rhodium complex **3a**: 0.28 g (0.36 mmol), 72% isolated yield. ^{11}B-NMR (64.2 MHz, ppm, $CDCl_3$); −1.72 (*s*, 1B, BF_4), −5.43 (*d*, 2B, J_{BH} = 140 Hz), −8.20 (*d*, 4B, J_{BH} = 150 Hz), −11.21 (*d*, 4B, J_{BH} = 150 Hz). ^{1}H-NMR (200.13 MHz, ppm, $CDCl_3$) 7.83 (*m*, 4H, PPH), 7.75 (*m*, 6H, PPH), 5.45 (br *s*, 4H = CH cod), 3.13 (*d*, 2H, N–CH_2, 2.60 Hz), 2.93 (*s*, 6H, NMe), 2.58 (br *s*, 4H, CH_{exo} cod), 2.34 (br *s*, 4H, CH_{endo} cod). $^{13}C\{^1H\}$-NMR (50.3 MHz, ppm, $CDCl_3$) 139.64 (PPH), 138.33 (PPH), 133.42 (PPH), 69.52 (*s* = CH cod), 55.27 (*s*, N–CH_2), 55.64 (*s*, NMe), 17.89 (*s*, CH_2 cod); $^{31}P\{^1H\}$-NMR (80.0 MHz, ppm, $CDCl_3$): 52.63 (*s*, PPh_2). Anal. Calc. for $C_{25}H_{40}B_{11}F_4NPIr$: C, 38.86; H, 5.22; N, 1.81. Found: C, 38.89; H, 5.25; N, 1.84%. Mp = 185–188°C (dec.). IR spectrum (KBr pellet, cm^{-1}) 2954 (m), 2924 (m), 2854 (m), 2568 (s), 2360 (m), 2340 (w), 1480 (w, sh), 1468 (s), 1436 (m), 1376 (m), 1312 (w), 1189 (w), 1053 (m, br), 884 (w), 745 (w), 700 (m), 670 (w), 517 (m).

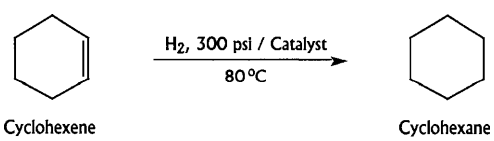

Scheme 4.

3.5. Reaction of *3a* with PPh_3 and CO

A solution of complex **3a** (0.14 g, 0.2 mmol) in toluene (10 ml) was treated with PPh_3 (0.16 g, 0.6 mmol) at r.t. for 5 min. The orange color of the solution quickly faded to give a brown–yellow solution. This was placed under an atmosphere of CO causing a color change to yellow. The NMR spectra of this sample showed complete conversion to $[(PPh_3)_2Rh(CO)_3]^+BF_4^-$ **4a**. The volatile substances were then removed in vacuo, and the resulting solid was extracted with CH_2Cl_2. The addition of hexane to the concentrated extract gave complex **4a** as yellow crystals. Yield: 0.14 g (0.18 mmol, 90%). ^{11}B-NMR (64.2 MHz, ppm, $CDCl_3$); −2.23 (*s*, BF_4). ^{1}H-NMR (200.13 MHz, ppm, $CDCl_3$) 7.64 (*m*, 4H, PPH), 7.58 (*m*, 6H, PPH). $^{13}C\{^1H\}$-NMR (50.3 MHz, ppm, $CDCl_3$) 188.87 (dt, Rh–CO, $^1J_{Rh-C}$ = 80.6 Hz, $^2J_{P-C}$ = 14.4 Hz), 135.44 (PPH), 132.77 (PPH), 128.74 (PPH). $^{31}P\{^1H\}$-NMR (80.0 MHz, ppm, $CDCl_3$): 21.83 (dm, PPh_2, J_{Rh-P} = 102.7 Hz). Anal. Calc. for $C_{39}H_{30}BF_4O_3P_2Rh$: C, 58.68; H, 3.79. Found: C, 58.66; H, 3.77%. M.p. = 154–156°C (dec.). IR spectrum (KBr pellet, cm^{-1}) 3066 (w), 2076 (s), 2025 (s), 1998 (s), 1460 (m), 1420 (s), 1220 (w), 1086 (s), 1054 (s), 1028 (s), 998 (m), 838 (w), 764 (w), 734 (m), 650 (m), 536 (w), 488 (s).

3.6. Reaction of *3b* with PPh_3 and CO

A similar procedure was employed as described above but with the following quantities: **3b** (0.16 g, 0.21 mmol); PPh_3 (0.16 g, 0.6 mmol). A yellow solid of $[(PPh_3)_2Ir(CO)_3]^+BF_4^-$ **4b** was isolated as described for

the rhodium complex **4a**: 0.17 g (0.19 mmol), 93% isolated yield. ^{11}B-NMR (64.2 MHz, ppm, $CDCl_3$); −1.98 (*s*, BF_4). ^{1}H-NMR (200.13 MHz, ppm, $CDCl_3$) 7.77 (*m*, 4H, PPH), 7.62 (*m*, 6H, PPH). ^{13}C{^{1}H}-NMR (50.3 MHz, ppm, $CDCl_3$) 172.8 (*t*, Ir–CO, $^2J_{P-C} = 9.4$ Hz), 133.99 (PPH), 132.77 (PPH), 129.02 (PPH). ^{31}P{^{1}H}-NMR (80.0 MHz, ppm, $CDCl_3$): 33.74 (PPh_2). Anal. Calc. for $C_{39}H_{30}BF_4IrO_3P_2$: C, 52.77; H, 3.41. Found: C, 52.74; H, 3.47%. Mp = 163–165°C (dec.). IR spectrum (KBr pellet, cm^{-1}) 3062 (w), 2074 (s), 2020 (s), 2000 (s), 1473 (m), 1422 (s), 1410(w), 1323 (w), 1218 (w), 1086 (s), 1050 (s), 1025 (s), 1000 (m), 840 (w), 760 (w), 740 (m), 623 (m), 520 (w), 500 (s).

3.7. General procedure for catalytic experiments

A solution of the catalyst (0.03 mmol) and cyclohexene (3.0 g, 36.5 mmol) in dried solvent (20.0 g) was stirred in an autoclave under a constant dihydrogen pressure (300 psi, 20 atm) at 80°C, for 50 min. After the required reaction time, the autoclave was cooled to r.t., the pressure was carefully released and the solution was passed through celite and analyzed by GC, GC–MS and ^{1}H-NMR spectroscopy. Conversions were determined by GC.

3.8. X-ray crystallography

Suitable crystals of **2**, **3a**·CH_2Cl_2, and **4a**·CH_2Cl_2 were obtained by the slow diffusion of hexane into a methylene chloride solution of the complexes at r.t. and were mounted on a glass fiber. Diffraction measurements were made on an Enraf CAD-4 automated diffractometer with graphite-monochromated Mo–K_α radiation. The unit cell was determined by using search, center, index and least-squares routines. The intensity data were corrected for Lorentz and polarization effects and for anisotropic decay. Each structure was solved by the application of direct methods using the SHELXL-86 program [19a] and least-squares refinement using SHELXL-93 [19b]. All nonhydrogen atoms were refined using anisotropic thermal parameters. All hydrogen atoms, including those on the cage B–H group and the hydrogens of the cod ligand, were located and refined using isotropic thermal parameters.

4. Supplementary material

Crystallographic data for the structural analysis have been deposited with the Cambridge Crystallographic Data Center, CCDC no. 148028 for compound **4a**, CCDC no. 148029 for compound **3** and CCDC no. 148030 for compound **2**. Copies of this data may be obtained free of charge from The Director, CCDC, 12 Union Road, Cambridge CB2 1EZ, UK (Fax: +44-1223-336033; e-mail: deposit@ccdc.cam.ac.uk or www:http://www.ccdc.cam.ac.uk).

Acknowledgements

Financial support by the BK-21 program from the Korean Ministry of Education is gratefully appreciated.

References

[1] (a) I. Takei, Y. Nishibayashi, Y. Arikawa, S. Uemura, M. Hidai, Organometallics 18 (1999) 2271. (b) M. Valentini, K. Selvakumar, M. Wörle, P.S. Pregosin, J. Organomet. Chem. 587 (1999) 244. (c) I.D. Kostas, C.G. Screttas, J. Organomet. Chem. 585 (1999) 1. (d) A. Jacobi, G. Huttner, U. Winterhalter, J. Organomet. Chem. 571 (1998) 231. (e) H. Yang, M. Alvarez-Gressier, N. Lugan, R. Mathieu, Organometallics 16 (1997) 1401. (f) H. Yang, N. Lugan, R. Mathieu, Organometallics 16 (1997) 2089. (g) Y. Hayashi, H. Sakai, N. Kaneta, M. Uemura, J. Organomet. Chem. 503 (1995) 143. (h) C.G. Arena, F. Nicolò, D. Drommi, G. Bruno, F. Faraone, J. Chem. Soc. Chem. Commun. (1994) 2251.

[2] (a) D.M. Roundhill, R.A. Bechtold, S.G.N. Roundhill, Inorg. Chem. 19 (1980) 284. (b) T.B. Rauchfuss, F.T. Patino, D.M. Roundhill, Inorg. Chem. 14 (1975) 652.

[3] (a) J.D. Lee, C.K. Baek, J. Ko, K. Park, S. Cho, S.K. Min, S.O. Kang, Organometallics 18 (1999) 2189. (b) Y. Kang, J. Ko, S.O. Kang, Organometallics 18 (1999) 1818. (c) Y.J. Lee, S.J. Kim, C.H. Kang, J. Ko, S.O. Kang, Organometallics 17 (1998) 1109. (d) Y. Kang, J. Lee, Y.K. Kong, J. Ko, S.O. Kang, J. Chem. Soc. Chem. Commun. (1998) 2343.

[4] (a) C. Viñas, M.A. Flores, R. Núñez, F. Teixidor, R. Kivekäs, R. Sillanpää, Organometallics 17 (1998) 2278. (b) F. Teixidor, M.A. Flores, C. Viñas, R. Kivekäs, R. Sillanpää, Angew. Chem. Int. Ed. Engl. 35 (1996) 2251. (c) B. Pirotte, A. Felekidis, M. Fontaine, A. Demonceau, A.F. Noels, J. Delarge, I.T. Chizhevsky, T.V. Zinevich, I.V. Pisareva, V.I. Bregadze, Tetrahedron Lett. 34 (1993) 1471. (d) J.A. Belmont, J. Soto, R.E. King III, A.J. Donaldson, J.D. Hewes, M.F. Hawthorne, J. Am. Chem. Soc. 111 (1989) 7475. (e) P.E. Behnken, J.A. Belmont, D.C. Busby, M.S. Delaney, R.E. King III, C.W. Kreimendahl, T.B. Marder, J.J. Wilczynski, M.F. Hawthorne, J. Am. Chem. Soc. 106 (1984) 3011. (f) P.E. Behnken, D.C. Busby, M.S. Delaney, R.E. King III, C.W. Kreimendahl, T.B. Marder, J.J. Wilczynski, M.F. Hawthorne, J. Am. Chem. Soc. 106 (1984) 7444. (g) T.E. Paxson, M.F. Hawthorne, J. Am. Chem. Soc. 96 (1974) 4674.

[5] R. Kivekäs, R. Sillanpää, F. Teixidor, C. Vinas, R. Nunez, Acta Crystallogr. Scand., Sect. C 50 (1994) 2027.

[6] (a) V.S. Mastryukov, O.V. Dorofeeva, L.V. Vilkov, Russ. Chem. Rev. 49 (1980) 1181. (b) V.S. Mastryukov, O.V. Dorofeeva, L.V. Vilkov, Usp. Khim. 49 (1980) 2377.

[7] I.C.M. Wehman-Ooyevaar, G.M. Kapteijn, D.M. Grove, W.J.J. Smeets, A.L. Spek, G. van Koten, J. Chem. Soc. Dalton Trans. (1994) 703.

[8] R.R. Schrock, J.A. Osborn, J. Am. Chem. Soc. 93 (1971) 2397.

[9] D.H.M.W. Thewissen, K. Timmer, J.G. Noltes, J.W. Marsman, R.M. Laine, Inorg. Chim. Acta 97 (1985) 143.

[10] T.B. Rauchfuss, F.T. Patino, D.M. Roundhill, Inorg. Chem. 14 (1975) 652.

[11] Y. Nishibayashi, K. Segawa, Y. Arikawa, K. Ohe, M. Hidai, S. Uemura, J. Organomet. Chem. 381 (1997) 545.

[12] (a) T. Yoshida, K. Tani, T. Yamagata, Y. Tatsuno, T. Saito, J. Chem. Soc. Chem. Commun. (1990) 292. (b) W.R. Cullen, F.W.B. Einstein, C.H. Huang, A.C. Willis, E.S. Yeh, J. Am. Chem. Soc. 102 (1980) 988.
[13] (a) W.J. Knebel, R.J. Angelici, Inorg. Chem. 13 (1974) 627. (b) W.J. Knebel, R.J. Angelici, Inorg. Chem. 13 (1974) 632. (c) W.J. Knebel, R.J. Angelici, O.A.Gansow, D.J. Darensbourg, J. Organomet. Chem. 66 (1974) C11.
[14] R.R. Scrock, J.A. Osborn, J. Am. Chem. Soc. 93 (1971) 2397.
[15] S.L. Randall, J.S. Thompson, L.A. Buttrey, J.W. Ziller, M.R. Churchill, J.D. Atwood, Organometallics 10 (1991) 683.
[16] T.L. Heying, J.W. Ager, Jr., S.L. Clark, D.J. Mangold, H.L. Goldstein, M. Hilman, R.J. Polak, J.W. Szymanski, Inorg. Chem. 2 (1963) 1089.
[17] G. Giordano, R.H. Crabtree, Inorg. Synth. 19 (1979) 218.
[18] J.L. Herde, J.C. Lambert, C.V. Senoff, Inorg. Synth. 15 (1974) 18.
[19] (a) G.M. Sheldrick, in: G.M. Sheldrick, C. Kruger, R. Goddard (Eds.), Crystallographic Computing 3, Oxford University Press, London, 1985, pp. 175–189. (b) G.M. Sheldrick, in: H.D. Flack, L. Parkanyi, K. Simon (Eds.), Crystallographic Computing 6, Oxford University Press, London, 1993, pp. 111–122.